The dynamics of bedform amalgamation: new insights from a very thin flume

Jim Best [1], Gianluca Blois [1], Julio Barros [1] and Kenneth Christensen [1]

1. University of Illinois, Urbana-Champaign, Illinois, USA
jimbest@illinois.edu; blois@illinois.edu; jmbarros@illinois.edu; ktc@illinois.edu

Abstract

Bedform superimposition and amalgamation are ubiquitous in many sedimentary environments and yet we possess a sparse knowledge of the fluid dynamics of such bedform interactions and both their sediment transport and morphological consequences. In this paper, we report on results concerning the morphology and flow fields of amalgamating *mobile* bedforms using a unique, narrow (5 mm wide) flume, which allows the behavior of strictly two-dimensional bedforms to be observed and quantified. Measurement of the morphology and flow fields associated with bedform amalgamation reveals the importance of interactions between the separation zones of the upstream and downstream bedforms, with flow sheltering, shear layer interactions, bedform stalling and leeside erosion being central to the amalgamation process. These fluid dynamic patterns reveal a distinct sequence of stages during bedform superimposition and amalgamation, which leave a characteristic record in the preserved sedimentary cross-strata.

1. BACKGROUND

Bedform superimposition and amalgamation are ubiquitous in all river and marine environments and lay behind the processes of bedform growth and diminution, and are also central to the preservation of the deposits of bedforms in the subsurface. Recent years have witnessed increased study of the interactions between bedforms, yet we still possess a rudimentary knowledge of the fluid dynamic interactions between bedforms under mobile bed conditions (Best, 2005). Research has shown how the dynamics of such bedform interactions may be critical across the transition from ripples to dunes (Bennett and Best, 1996; Robert and Uhlman, 2001; Schindler and Robert, 2004, 2005), Additionally, experimental work has indicated that the interactions of two bedforms may produce non-linear effects in the production of turbulence in the bedform leeside, with the interactions between the shear layers produced from adjacent leeside separation zones being critical (Fernandez et al., 2006; Palmer et al.,

2011). Recent research documenting the interactions between barchan dunes (Schwämmle and Herrmann, 2003; Endo et al., 2004; Hersen and Douady, 2005; Duran et al., 2005, 2007; Hugenholtz and Barchyn, 2012) has also shown the complex behaviour of such interactions, and that these dynamics may produce a range of kinematic characteristics in dune evolution and migration (Schwämmle and Herrmann, 2003; Endo et al., 2004). Additionally, recent work documenting the cross-stratification produced by bedforms (Reesink and Bridge, 2007, 2009) has pointed to the importance of bedform superimposition and amalgamation in controlling the geometry and internal structure of bedding produced by a range of different size bedforms, from ripples to larger bar forms in rivers.

Such experimental studies are often made more complex due to the 3D nature of mobile bedforms, which makes quantification of their flow fields difficult, if not impossible, especially in the leeside region when superimposition and amalgamation are occurring and are strongly 3D processes.

2. METHODOLOGY

In order to examine the interactions between bedforms, we constructed a 5 mm wide flume (Fig. 1) that is designed to remove any three-dimensionality in the bedform planform, and thus allow interactions between 2D bedforms to be investigated and quantified. The working section of the flume is 3.0 m long, 0.25 m high and 0.005 m wide. A distribution plenum, fabricated of clear acrylic, guides fluid into the working section, whilst a return plenum collects the flow at the downstream end of the working section. An acrylic roof is fitted to the top of the flume to provide support and maintain the width of the channel throughout its length. An integral sediment trap funnels any sediment down into the return piping where it is recirculated back to the inlet section. The water and sediment circulation is driven by a magnetic drive, glass fiber reinforced polypropylene, centrifugal pump. An inline electromagnetic flow meter in the return line provides a real-time display of discharge, with values being adjustable from *c.* 3 to 48 L min^{-1}(*c.* 50-800 cm^{3}s^{-1}). An acrylic stop-gate is inserted at the end of the flume to provide a control on the thickness of the sediment bed and help set the flow depth. The required flow depth and velocity are thus controlled by selecting the appropriate volume of water within the flume and the pumped discharge. The entire flume is mounted on a steel framework that provides both support and allows the flume slope to be adjusted via a jack at the inlet end of the flume. Adjustment of the slope thus allows a constant flow depth to be imposed along the entire test section.

The sediment used in these experiments consisted of 212-325 μm soda lime glass beads (density 2.47 g cm^{-3}) that formed a bed *c.* 5 cm thick along the entire length of the flume. A small quantity of 150 μm mean diameter silica carbide (density 3.2 g cm^{-3}) sand was added to the mixture during the experiments to aid visualization of the cross-stratification produced by the migrating bedforms. A flow depth of *c.* 0.13 m was employed in these experiments with a discharge of 23.6 L min^{-1} yielding a mean velocity in the test section of *c.* 0.59 ms^{-1}. Measurements of the bedform profiles were taken using cameras mounted at the side of the flume. A Nikon D90 DSLR was used with a remote control timer to take images every 5 s, whilst the PIV camera (see below) was also used to provide a record of the changing bed elevation through time. These images were used to examine the geometrical characteristics of the bedforms, including their height, wavelength and shape, and migration celerity and characteristics. A grey-level thresholding scheme was found to well capture the profiles of the bedforms as they evolved through time (Fig. 2).

In addition to this morphological study, particle image velocimetry (PIV) was used to quantify the flow fields during bedform growth, superimposition and amalgamation. PIV permits study of the mutual interactions between the flow field and mobile bed in all phases of bedform development. A dual-cavity Nd:YAG laser (15 Hz and 35 mJ per pulse) was used to project a 0.5 mm thick light sheet, through a series of mirrors, into the working section of the flume. This allowed illumination of an area *c.* 200 mm × 200 mm. Neutrally-buoyant 10 μm diameter fluorescent particles (emission approx. 670 nm – LeFranc & Bourgeois Flashe Light Orange) were introduced into the flow and the light scattered by these particles was collected by a 12-bit, frame-straddle CCD camera (11 Mpixel) coupled with a 60 mm focal-length lens and high-pass filter (cutoff at 650 nm). This set-up allowed us to selectively collect the light from the tracer particles and filter out the light from the suspended sediment that was significant in the lee side of the bedforms. Sequences of images were collected at a rate of 2 Hz. Pre-processing of these images involved the development of dynamic masking procedures based upon detection of the position of the bedform. Interrogation of these images was performed using recursive cross-correlation techniques and adaptive interrogation windows to maximize the spatial resolution of the associated instantaneous velocity fields. Post-processing of the data set involved detection of the flow fields associated with specific stages of bedform evolution that allowed production of maps of downstream and vertical velocities, turbulence intensities and vorticity.
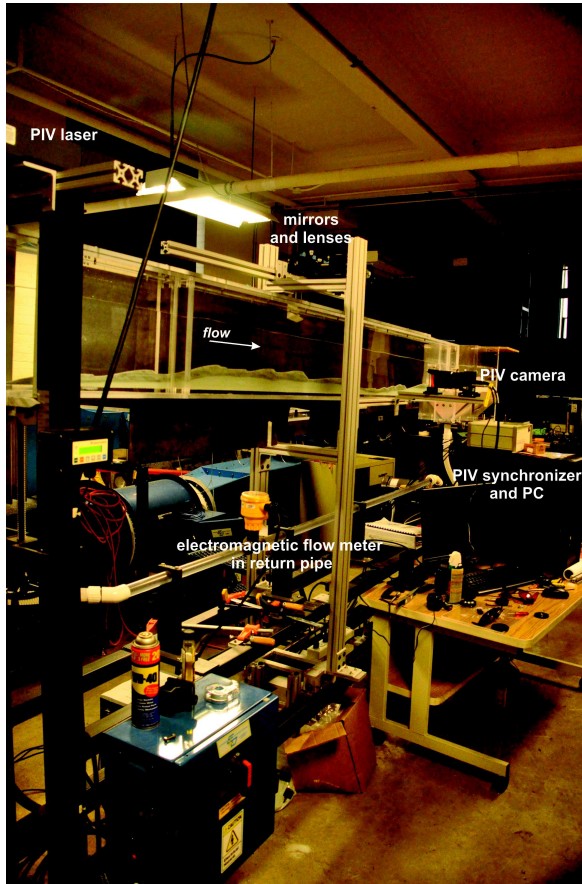
Figure 1. The 5 mm wide flume with the PIV laser and camera installed. Flow is away from the observer.

3.   RESULTS

In this paper, we will detail the interactions between ripples migrating within the flume, and document the changing flow fields during superimposition and amalgamation of mobile bedforms. We will use these observations to propose a model for flow as bedforms become superimposed and amalgamate, and to detail the internal stratification such processes produce.

The superimposition of ripples in the flume involves five principal stages: 1) initial migration of a smaller, larger celerity, upstream ripple that initially has little or no fluid dynamic influence on the downstream bedform (Fig 2A); 2) As the smaller ripple migrates up the stoss side of the downstream form, the leeside flow separation zone of the upstream form begins to exert a sheltering effect on the downstream bedform (Figure 2B). This results in both less sediment being transported

to the downstream bedform, as it is trapped by the upstream ripple, and also lower flow velocities over the crest of the downstream bedform. Both of these factors serve to decrease the celerity of the downstream bedform; 3) As the upstream bedform continues to migrate and catch the downstream bedform, its flow separation zone, and erosion at its reattachment region, begins to erode the crest of the downstream bedform (Fig. 2C). This produces an erosion surface over which the upstream bedform migrates, and lowers the height of the downstream bedform; 4) Bedform migration continues upon the now essentially static and stalled downstream bedform (Fig. 2D) and leads to eventual amalgamation of the two bedforms (Figure 2E). This resultant bedform now possesses a larger and renewed flow separation zone, and this amalgamated bedform then begins to migrate downstream (Fig. 2E). This amalgamation process thus produces a distinct reactivation surface between the lower and upper cross-stratification produced by these two bedforms, with this surface being the product of bedform amalgamation and not any change in mean flow conditions; 5) The process may then begin again with the stoss side migration of another smaller upstream ripple (Fig. 2F).

Results from the PIV show the changing patterns of flow around bedforms during their migration, with the high resolution data showing the details of flow near the bed as well as in the bedform leeside. A sequence of four images (Fig.3) shows flow around a migrating bedform that is in the initial stages of superimposition. Initial migration of the bedform (Figs 3A,B) shows no influence of an upstream bedform, with a region of maximum streamwise velocity over the crest, a marked region of flow separation in the leeside with recirculating flow, a strong shear layer surrounding this region and reattachment on the toe of the bedform. The presence of an advancing superimposed bedform is shown by the appearance of a lower velocity region upstream (Fig. 3C), a result of an upstream bedform wake, that begins to both decrease velocities at the crest and also decrease the size of the flow separation zone. Continued migration of this bedform, whose morphology is not seen in this sequence, begins to allow erosion of the crest of the downstream bedform (Fig. 3D) and shows an advancing lower-

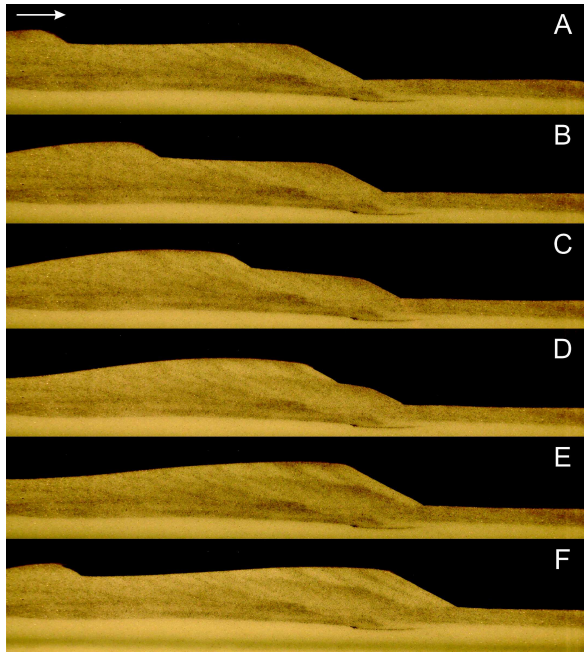velocity wake region on the stoss side of the bedform.

Figure 2. Images of ripples imaged through the flume sidewalls. These six images are each 20 s apart (total sequence = 100 s) and show the superimposition and eventual amalgamation of a smaller ripple with an initially larger downstream bedform. The ripple height is *c.* 1.5 cm. Flow left to right.

Plots of the flow field during another instance of bedform superimposition show a similar sequence of events, in maps of changing streamwise velocity (Fig. 4) and spanwise vorticity (Fig. 5). Initial migration of the bedform shows a larger leeside flow separation zone (Figs 4A,B) and associated spanwise vorticity along the shear layer (Figs 5A,B). The separation zone becomes smaller (Figs 4C,D,E) as an upstream bedform approaches, with the shear layer also becoming less extensive (Figs 5D,E). Impingement of the shear layer from the upstream bedform onto the stoss side of the downstream ripple (Figs 4D,E,F and 5D,E,F) results in erosion of this surface and a decrease in the bedform height.
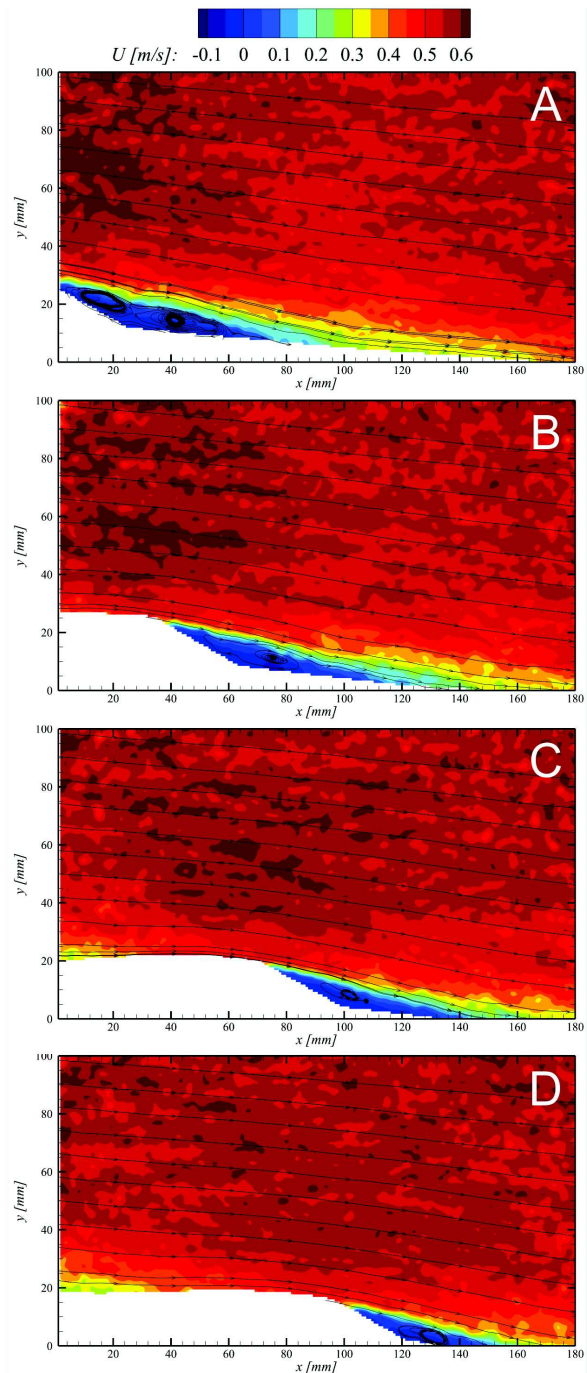

Figure 3. Instantaneous PIV flow field maps showing streamwise flow velocity (in ms^{-1}) and streamlines over a migrating bedform (A,B) that begins to show the influence of an upstream superimposed bedform (C,D). Flow fields are 15 s apart and the ripple height is *c.* 2 cm. Flow left to right.
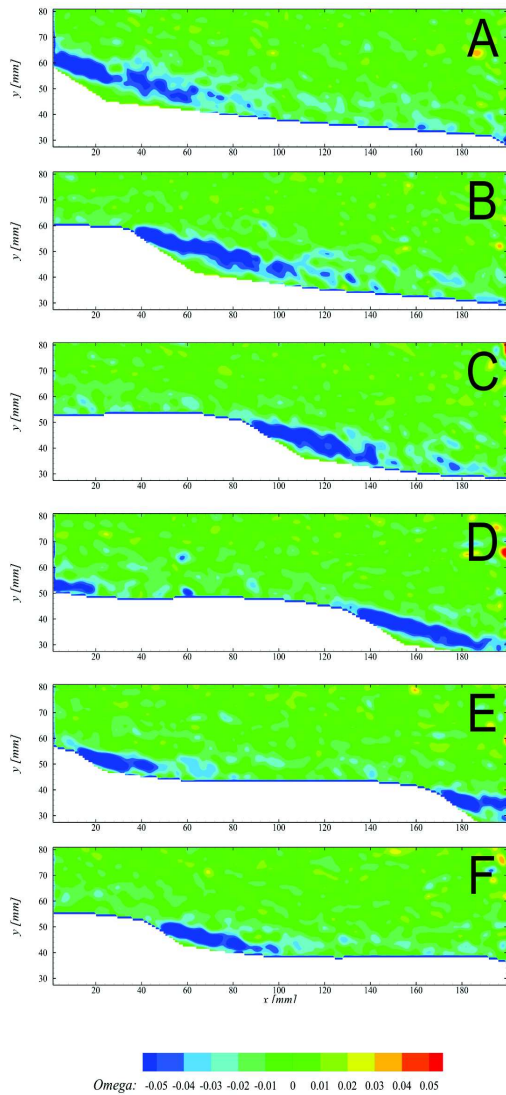
Omega: -0.05 -0.04 -0.03 -0.02 -0.01 0 0.01 0.02 0.03 0.04 0.05

U [ms^{-1}]: -0.05 0 0.05 0.1 0.15 0.2 0.25 0.3 0.35 0.4 0.45 0.5 0.55 0.6

Figure 4. Instantaneous PIV flow field maps showing streamwise flow velocity (in ms^{-1}) over a migrating bedform (A,B,C) that has a superimposed bedform migrating over its stoss side (D,E,F). Note the change in the size of the separation zone associated with the downstream bedform as the upstream ripple approaches (C,D,E), and that the impingement of the shear layer from the upstream bedform upon the bed causes erosion and lowering of the stoss side of the downstream bedform (D,E,F). Flow fields are 20 s apart and the ripple height is *c.* 1.5 cm. Flow left to right.
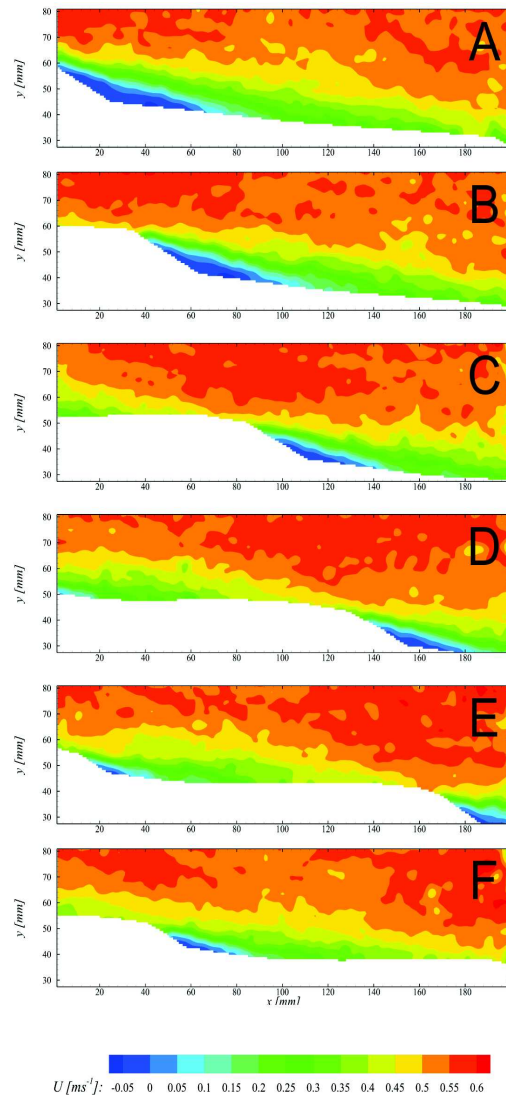
Figure 5. PIV flow field maps showing instantaneous spanwise vorticity over a migrating bedform (A,B) that has a superimposed bedform migrating over its stoss side (D,E,F) for the same realizations as shown in Figure 4. Flow fields are 20 s apart and the ripple height is *c.* 1.5 cm. Flow left to right.

4. REFERENCES

Bennett, S.J. and Best, J.L. (1996) Mean flow and turbulence structure over fixed ripples and the ripple-dune transition, in *Coherent Flow Structures in Open Channels*, edited by P. J. Ashworth et al., pp. 281– 304, John Wiley, Hoboken, N. J.

Best, J. 2005. The fluid dynamics of river dunes: A review and some future research directions. *Journal of Geophysical Research F: Earth Surface,* 110, F04S02.

Durán, O., Schwämmle, V. and Herrmann, H.J. (2005) Breeding and solitary wave behavior of dunes, *Phys. Rev. E*, 72, 021308, doi:10.1103/PhysRev E.72.021308.

Durán, O., Schwämmle, V., Lind, P.G. and Herrmann H.J. (2011) Size distribution and structure of barchan dune fields, *Nonlinear Processes Geophys.*, 18, 455–467, doi:10.5194/npg-18-455-2011.

Endo, N., Taniguchi, K. and Katsuki, A. (2004) Observation of the whole process of interaction between barchans by flume experiments, *Geophys. Res. Lett.,* 31, L12503, doi:10.1029/2004GL020168.

Fernandez, R., Best, J. and Lopez, F. (2006) Mean flow, turbulence structure and bedform superimposition across the ripple-dune transition, *Water Res. Research,* 42, W05406, doi:10.1029/2005WR 004330.

Hersen, P. and Douady, S. (2005) Collision of barchan dunes as a mechanism of size regulation, *Geophys. Res. Lett.,* 32, L21403, doi:10.1029/2005GL024179.

Hugenholtz, C.H. and Barchyn, T.E. (2012) Real barchan dune collisions and ejections, *Geophys. Res. Lett.,* 39, L02306, doi:10.1029/2011GL050299.

Palmer, J. A., Meja-Alvarez, R., Best, J.L. and Christensen, K.T. (2012) Particle-image velocimetry measurements of flow over interacting barchans dunes, *Exp. Fluids*, 52, 809-829, doi:10.1007/s00348-011-1104-4.

Reesink, A.J.H. and Bridge J.S. (2007) Influence of superimposed bedforms and flow unsteadiness on formation of cross strata in dunes and unit bars*, Sed. Geology*, 202, 281-296.

Reesink, A.J.H. and Bridge J.S. (2009) Influence of bedform superimposition and flow unsteadiness on the formation of cross strata in dunes and unit bars — Part 2, further experiments, *Sed. Geology*, 222, 274-300, 10.1016/j.sedgeo.2009.09.014.

Robert, A., and Uhlman, W. (2001) An experimental study on the ripple dune transition, *Earth Surf. Processes Landforms*, 26, 615– 629.

Schindler, R.J. and Robert, A. (2004) Suspended sediment concentration and the ripple-dune transition, *Hydrol. Processes*, 18, 3215–3227.

Schindler, R.J. and Robert, A. (2005) Flow and turbulence structure across the ripple-dune transition: An experiment under mobile bed conditions, *Sedimentology*, 52, doi:10.1111/j.1365-3091.2005.00706x.

Schwämmle, V. and Herrmann, H. J. (2003) Solitary wave behaviour of sand dunes, *Nature*, 426, 619– 620, doi:10.1038/426619a.